Published in : Advanced Steel Construction (2022), vol. 18, no.3, pp. 679-686
DOI:10.18057/IJASC.2022.18.3.5
Status : Postprint (Author's version)

CHARACTERISATION OF THE BEHAVIOUR OF BEAM-TO-COLUMN STEEL JOINTS UP TO FAILURE

Tudor Golea *, Jean-Pierre Jaspart and Jean-François Demonceau

Urban and Environmental Engineering, University of Liège, Liège, Belgium
** (Corresponding author: E-mail: tudor.golea@uliege.be)*

Abstract

The design of steel joints is currently dealt with in Eurocode 3 through the well-known "component method". In particular, Part 1-8 of this standard provides guidance on how to apply the method to a wide range of joint configurations allowing to assess the latter's initial rotational stiffness and resistance. Nonetheless, whenever a global structural plastic analysis is contemplated, provisions of Eurocode 3 are insufficient since no clear guidance on how to determine the ultimate resistance and the ultimate rotation capacity of joints is provided. In this paper, the full-range behaviour of beam-to-column steel joints is investigated using experimental, analytical, and numerical methods. A new analytical approach based on the component method is proposed and validated against five physical experiments. Through additional analytical expressions for the characterisation of basic components of steel joints, the proposed approach extends the applicability of the component method such that strain-hardening and ductility of components are accounted for. The results show a good agreement between the analytical prediction and the experimental results and also highlight specific limitations of the classical component method. Three-dimensional finite element (FE) models are also employed to simulate the behaviour of the tested beam-to-column joints. The results prove the accuracy of numerical models to simulate the non-linear response of steel joints emphasizing, however, the importance of proper modelling assumptions.

Keywords

Steel joints; Experimental tests; Component method; Finite element analysis; Steel structures

1. Introduction

In steel framed structures, beam-to-column joints were conventionally assumed to behave either as ideally pinned or fully rigid. This simplifying assumption was driven by the difficulty to characterise the behaviour of such joints and was widely accepted as a rule of good practice meant to ease the structural analysis and the design processes. Although its practical conveniences are undeniable, this simplification disregards the fact that most of the joints can be classified as semi-rigid, exhibiting in reality a finite stiffness. To overcome this limitation, considerable research efforts have been invested. The use of complex non-linear FE analyses may be seen as a solution for such purposes but, most of the times, it implies a tremendous computational effort which is not compatible with the daily practice in design offices. Accordingly, most of the research efforts have been dedicated to the derivation of practical tools and procedures to predict the behaviour of

Published in : Advanced Steel Construction (2022), vol. 18, no.3, pp. 679-686
DOI:10.18057/IJASC.2022.18.3.5
Status : Postprint (Author's version)

semi-rigid joints. In particular, a simple approach based on mechanical analytical models has been proposed, known nowadays as the "component method" [1]–[3].

Validated throughout extensive experimental campaigns, the component method proved to be a robust tool allowing to predict the strength and the initial stiffness of steel joints. In this regard, it has been implemented in Eurocode 3 [4] as a practical solution to be used by designers in global structural analyses of semi-rigid frames where the rotational behaviour of joints becomes an additional variable. Part 1-8 of this standard deals with the application of the component method, providing a comprehensive set of design rules that enables the designer to derive the moment-rotation curve $M_j - \phi$ for a variety of joint configurations. In general terms, the joint is considered as a set of individual basic components which, based on their mechanical properties, may have significant or negligible contributions to the overall behaviour of the joint. The contribution of each basic component is accounted for through an assembly procedure that assists the practitioner in the evaluation of the initial rotational stiffness $S_{j,ini}$ and the bending plastic design resistance $M_{j,Rd}$ of the joint. These two parameters are used further to generate a simplified $M_j - \phi$ curve which is rather an idealisation of the actual one since there is no ultimate bending resistance M_{Ru} or strain-hardening (post-plastic) stiffness $S_{j,st}$ taken into account. Therefore, this simplification comes at the expense of the ability to predict the actual response of the joints up to their failure while this ability of prediction is of great interest when considering the robustness of structure which is part of the normative requirements imposed by modern codes and standards [5]–[7].

Hereinafter, a general approach proposed by Jaspart et al. [8] is used to estimate the full $M_j - \phi$ curve of beam-to-column steel joints. This approach can be seen as an extension to the component method integrated in the current version of Eurocode 3. The analytical expressions provided in the European normative document are used to characterise the behaviour of the joints up to their plastic bending capacity. For the post-plastic behaviour, analytical expressions proposed after studies on numerous test results [1] are employed in the evaluation of the strain-hardening stiffness of the basic joint components.

Procedures for the evaluation of the post-plastic stiffness $S_{j,st}$, the ultimate bending resistance M_{Ru} and the ultimate rotation capacity ϕ_u are introduced. Based on these key parameters, the $M_j - \phi$ curve is estimated up to the failure of the joints, thus making possible to predict their full non-linear behaviour.

The experimental campaign conducted at the University of Liège within the research project RobustImpact [9] serves as a reference database for this paper. Five physical specimens of double-sided beam-to-column joints were tested under quasi-static loading conditions. The test specimens consisted of two I-section beams connected to an H- or I-section column. The fastening between these members was ensured through end-plates and high-strength bolts for three of the specimens, whilst for the other two, the beams were welded directly to the column. Throughout the tests, failure occurred in distinct basic components.

2. Experimental programme

2.1. Test setup

The experimental programme, including the test setup, was thoroughly presented by Demonceau et al. [10]. A schematic view of the experimental setup is illustrated in Fig. 1; a detailed presentation of the specific instrumentation used to acquire the experimental data is to be found in [11]. The double-sided

Published in : Advanced Steel Construction (2022), vol. 18, no.3, pp. 679-686
DOI:10.18057/IJASC.2022.18.3.5
Status : Postprint (Author's version)

beam-to-column joints were subjected to a monotonic load applied at the top of the column. A hydraulic jack was used to apply the load up to the failure of the joints. Several loading-unloading cycles were performed in order to identify the actual stiffness of the specimens. The displacements and deformations were tracked using displacement transducers and extensometers placed along the beams and at the level of the load application point. To simulate the support conditions corresponding to a simply supported element, a specific system that accommodates horizontal displacements and rotations was designed.

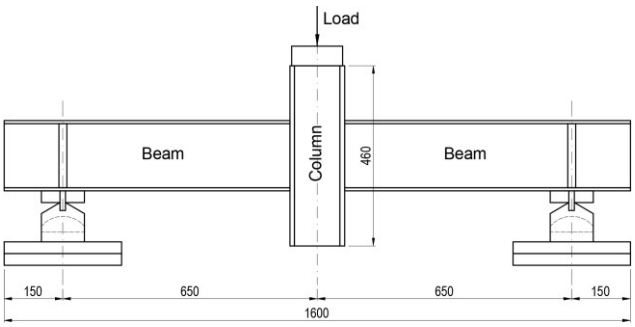

Fig. 1 Elevation view of the test setup

2.2. Test specimens

The global dimensions of the specimens were imposed by the limitations of the available laboratory setup. The length of the beams was chosen such that the specimen does not exceed a length of 1.6 m as depicted in Fig. 1. The specimens consisted of two IPE 180 sections that served as beams and a HEB 140 or an IPE 180 section representing the column. Three out of five specimens were designed and manufactured having bolted end-plate connections, whilst the other two were manufactured as joints with welded connections. All sections and end-plates were of steel grade S355. A total of eight M16 bolts of grade 10.9 were used for each joint with bolted end-plate connections. To ensure an adequate diffusion of transverse compression and tension forces transferred from the beams to the column, the length of the column was set at the value of 460 mm.

A summary of the main characteristics of the experimental specimens is reported in Table 1. A detailed view of their general layout is provided in Fig. 2. The first specimen named RJ (Real Joint) was designed as a reference joint configuration. From this actual joint configuration, four others were derived by modifying the geometrical properties or by providing additional stiffening elements with the objective of investigating the behaviour of several basic components from the Real Joint in isolation; accordingly, these adjustments were performed in such a way that the failure of only one basic component of the joint would occur. The specimens are identified through a specific label that corresponds to the failing basic component of the considered specimen: EPB for End-Plate in Bending, CFB for Column Flange in Bending, BFC for Beam Flange in Compression and CWC for Column Web in Compression.

Published in : Advanced Steel Construction (2022), vol. 18, no.3, pp. 679-686
DOI:10.18057/IJASC.2022.18.3.5
Status : Postprint (Author's version)

Table 1
Characteristics of specimens

Specimen	Connection type	Column section	Beams section	End-plate
RJ	Bolted end-plate	HEB 140	IPE 180	120x210x15
EPB		HEB 140	IPE 180	120x210x8
CFB		HEB 140	IPE 180	120x220x18
BFC	Welded	HEB 140	IPE 180	-
CWC		IPE 180	IPE 180	-

2.3. material tests

Quasi-static uniaxial tension tests were performed on coupons extracted from the end-plates and from the flanges/web of the IPE and HEB sections. A detailed report on the coupon tests and the stress-strain curves (σ_{eng} - ε_{eng}) of the steel material may be found in [11]. The main actual mechanical properties of the materials acquired from the tests are summarised in Table 2.

Table 2
Mechanical properties of materials

Element	Coupon	f_y [MPa]	ε_y [%]	f_u [MPa] End	ε_u [%]
IPE 180	Flange	413.3	1.97	537.7	21
	Web	435.5	2.07	545.2	25
HEB 140	Flange	385.3	1.83	539.6	20.6
	Web	433.7	2.06	544	22
End-plates	8 mm	409.3	1.95	594.8	185
	15 mm	416.6	1.98	588.7	23
	18 mm	384.5	1.83	556.2	22

The mechanical properties of the bolts material were not evaluated experimentally. However, tests on coupons from similar bolts of grade 10.9 were performed within the same research project. The values reported for the yield strength f_{yb}=1020 MPa and the ultimate strength f_{ub}=1080 MPa are taken as reference parameters for the computations carried out in the present paper.

3. Component method

3.1. Principles of the method

The component method emerged as a solution to the demand of practitioners seeking the influence of the behaviour of structural joints on the response of building frames. The method uses a hybrid analytical-mechanical approach to derive the $M_j—\phi$ curve of steel or steel-concrete composite joints.

Published in : Advanced Steel Construction (2022), vol. 18, no.3, pp. 679-686
DOI:10.18057/IJASC.2022.18.3.5
Status : Postprint (Author's version)

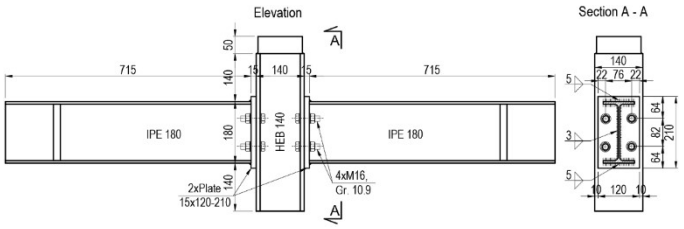

(a) RJ specimen

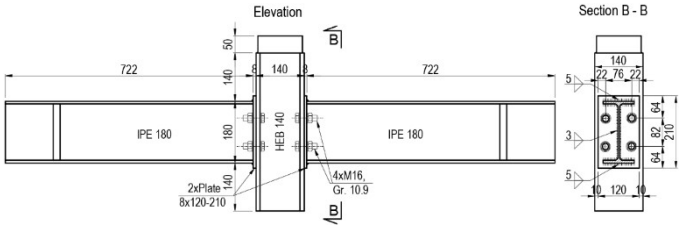

(b) EPB specimen

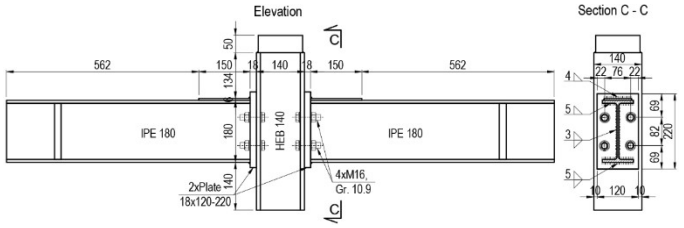

(c) CFB specimen

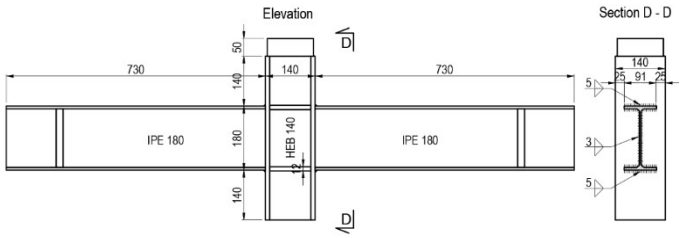

(d) BFC specimen

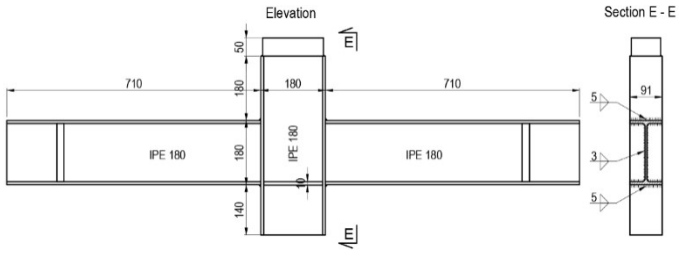

(d) CWC specimen

Fig. 2 Detailed views of the specimens

This is achieved by considering the joint as a set of individual basic components. Each of these components represents a part of the joint and is modelled as an extensional spring with mechanical properties (strength and stiffness) depending on the loading type. The full model of a joint comprises all these springs combined with infinitely rigid pin-ended elements. Some of the components may have contributions for both resistance and stiffness of the joint; these are identified as elastic-plastic components, whereas the ones

Published in : Advanced Steel Construction (2022), vol. 18, no.3, pp. 679-686
DOI:10.18057/IJASC.2022.18.3.5
Status : Postprint (Author's version)

contributing only to the resistance are labelled as rigid-plastic components. For the sake of exemplification, Fig. 3 illustrates the mechanical model of the RJ specimen investigated in this paper.

The components contributing to the overall response of the joints are associated with three distinctive zones - compression, tension, and shear zones. In this study, the investigated joints are symmetrically loaded, hence there is no shear action in the column web panel; so, the shear zone is disregarded in this particular case. Consequently, the relevant components are identified for the two zones as follows:

- compression zone: column web in compression (cwc) and beam flange in compression (bfc);
- tension zone: column web in tension (cwt), column flange in bending (cfb), bolts in tension (bt), end-plate in bending (epb) and beam web in tension (bwt).

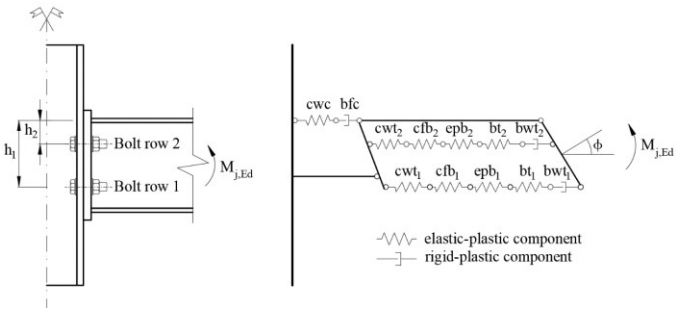

Fig. 3 Mechanical model of the RJ specimen

Relying on the mechanical properties of these basic components, the initial stiffness $S_{j,ini}$ and the plastic moment resistance M_{Rpl} of the joint are estimated through an assembly procedure. To accomplish this, a comprehensive three-step procedure is envisaged [2]:

1. identification of the active components in the investigated joint;
2. evaluation of mechanical properties in terms of stiffness and/or strength for each active component;
3. assembly of all the components and evaluation of the stiffness and/or resistance characteristics of the whole joint.

Eurocode 3 Part 1-8 provides rules and analytical expressions to characterise a variety of components in terms of stiffness and strength. The information available on the characterisation of components and on assembly procedures allows to cover a wide range of joint configurations and, for common design practice, it is generally sufficient to satisfy the needs of practitioners.

3.2 Application of the component method

3.2.1. Characterisation of active components

The level of refinement of the component method is highly dependent on the accuracy of the components characterisation. In this regard, the stiffness, the strength, and the deformation capacity of components may be derived using various techniques with different levels of accuracy and complexity such as experimental testing, numerical simulations, and analytical methods.

Herein, the analytical expressions provided in Eurocode 3 Part 1-8 are used to derive the mechanical properties of the basic components. Prior to their actual characterisation, the active components of the joints are identified as suggested by the first step of the component method. Table 3 lists the basic

Published in : Advanced Steel Construction (2022), vol. 18, no.3, pp. 679-686
DOI:10.18057/IJASC.2022.18.3.5
Status : Postprint (Author's version)

components activated in the five joints investigated within this paper. The contribution of each active component to the overall resistance or stiffness of the joint is marked correspondingly.

All the active components being identified, their characterisation in terms of resistance, stiffness, and deformation capacity is contemplated. This implies the definition of force-deformation F-Δ curves for the extensional springs simulating the behaviour of the actual components. The classic approach proposed in Eurocode 3 enables the user to define an elastic-perfectly plastic F-Δ curve for each active component as depicted in Fig 4 (a). Therefore, the components are considered to deform elastically up to their plastic resistance and, if no brittle failures nor instability phenomena occur, they may deform plastically to the extent of their deformation capacity.

The assumption of considering an elastic-perfectly plastic model leads to a conservative prediction of the overall behaviour of the joints. Potential strainhardening effects and membrane effects are simply disregarded, defining thus the post-plastic behaviour as a yield plateau without a well-specified limit. To overcome this limitation and to enhance the accuracy of the analytical prediction, emphasis has shifted towards the characterisation of the post-plastic response of basic joint components. Based on studies of numerous test results, Jaspart et al. [8] proposed analytical expressions for the evaluation of the strain-hardening stiffness of various basic components. Consequently, the full non-linear response of components may be defined through simplified bi-linear F-Δ curves describing the elastic and the post-plastic behaviour as shown in Fig. 4 (b) Therefore, the ductility of components, roughly and only partially addressed in the present version of Eurocode 3, becomes a quantifiable characteristic.

Table 3

Basic active components in the investigated joints

Component	RJ, EPB and CFB		BFC and CWC	
	Resistance	Stiffness	Resistance	Stiffness
Column web in compression	✓	✓	✓	✓
Column web in tension	✓	✓		
Column flange in bending	✓	✓		
End-plate in bending	✓	✓		
Beam flange in compression	✓	*	✓	*
Beam web in tension	✓	*		
Bolts in tension	**	✓		

* The contribution of the component is accounted for in the deformation of the beam;
** The contribution of the component is accounted for in the equivalent T-stub model.

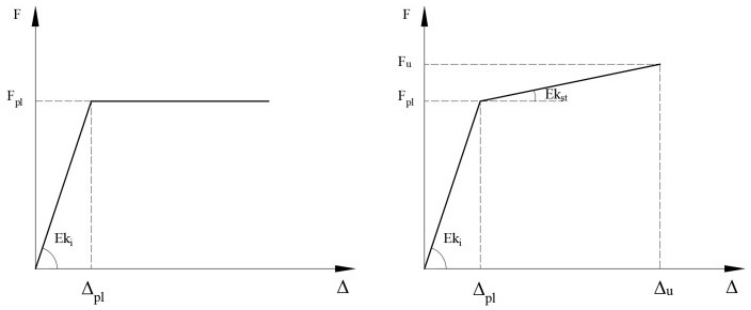

(a) F-Δ curve according to Eurocode 3 (b) F-Δ curve proposed by Jaspart et al [8]

Fig. 4 Characterisation of components through force-deformation curves

Published in : Advanced Steel Construction (2022), vol. 18, no.3, pp. 679-686
DOI:10.18057/IJASC.2022.18.3.5
Status : Postprint (Author's version)

Analytical expressions proposed in Eurocode 3 Part 1-8 are used to estimate the plastic resistance F_{Rpl} and the initial stiffness coefficients k_i of basic components. A brief survey of these is provided in Table 4 covering all the components of interest within the scope of this paper.

Table 4

Basic active components in the investigated joints

Component	Plastic resistance	Stiffness coefficient
Column web in compression	$F_{c,wc,Rd} = \frac{\omega k_{wc} b_{eff,c,wc} t_{wc} f_{y,wc}}{\gamma_{M0}}$ but $F_{c,wc,Rd} \leq \frac{\omega k_{wc} p b_{eff,c,wc} t_{wc} f_{y,wc}}{\gamma_{M1}}$	$k_2 = \frac{0.7 b_{eff,c,wc} t_{wc}}{d_c}$
Column web in tension	$F_{t,wc,Rd} = \frac{\omega b_{eff,t,wc} t_{wc} f_{y,wc}}{\gamma_{M0}}$	$k_3 = \frac{0.7 b_{eff,t,wc} t_{wc}}{d_c}$
Column flange in bending	* Equivalent T-stub model	$k_4 = \frac{0.9 l_{eff} t_{fc}^3}{m^3}$
End-plate in bending	* Equivalent T-stub model	$k_5 = \frac{0.9 l_{eff} t_p^3}{m^3}$
Beam flange in compression	$F_{c,fb,Rd} = \frac{M_{c,Rd}}{h - t_{fb}}$	$k_7 = \infty$
Beam web in tension	$F_{t,wb,Rd} = \frac{b_{eff,t,wb} t_{wb} f_{y,wb}}{\gamma_{M0}}$	$k_8 = \infty$
Bolts in tension	$F_{t,Rd} = \frac{0.9\, f_{ub} A_s}{\gamma_{Mb}}$	$k_{10} = \frac{1.6 A_s}{L_b}$

* The reader is asked to refer to the T-stub model addressed in EN 1993-1-8

The post-plastic behaviour of the active components is evaluated as proposed in [8]. The ultimate resistance is simply estimated by substituting the yield strength of steel f_y by the ultimate strength f_u in the formulae listed in Table 4. The strain-hardening stiffness coefficients k_{st} are estimated on the basis of k_i as follows in Eq. (1). This expression is valid only for such components as the column web in compression (cwc), column web in tension (cwt), column flange in bending (cfb), and the end-plate in bending (epb), i.e. for components which can exhibit a ductile behaviour.

$$k_{st} = \frac{E_{st}}{E} k_i \tag{1}$$

In Eq. (1), k_i is the initial stiffness coefficient of the component, E is the modulus of elasticity of steel and E_{st} is the strain-hardening modulus in the steel σ-ε curve. As proposed in [1], the ratio E_{st}/E is taken as 1/50 for all components contributing to the strain-hardening stiffness.

3.2.2. Moment resistance

Eurocode 3 suggests an assembly procedure for the estimation of the design moment resistance of joints. In general lines, the assembly procedure allows to derive the mechanical properties of the whole joint from those of the active basic components. This implies the fulfilment of the static theorem by determining the distribution of internal forces so that the equilibrium with the external forces acting on the joint is satisfied. Additionally, this internal distribution of forces has to account for the behaviour of the components under

Published in : Advanced Steel Construction (2022), vol. 18, no.3, pp. 679-686
DOI:10.18057/IJASC.2022.18.3.5
Status : Postprint (Author's version)

specific loading, ensuring the displacement compatibility (kinematic theorem) with respect to the stiffness, the resistance, and the ductility of components.

The plastic bending resistance of a joint M_{Rpl} is associated to the plastic resistance F_{Rpl} of the weakest individual joint component of each activated row. If there is no axial force to be transferred to the joint from the connected member, the plastic flexural resistance is estimated based on the following equilibrium equation:

$$M_{Rpl} = \sum_{r} h_r F_{tr,Rpl} \tag{2}$$

where $F_{tr,Rpl}$ is the plastic resistance of the row r, h_r is the distance from the row r to the centre of compression, and r is the row number. For joints with bolted connections, r stands for the number of bolt rows in tension, whereas for welded connections, only one row in tension can be identified - located at the level of the column web in tension component.

The plastic resistance of a bolt row is taken as the minimum of the resistances of components active at the level of row r as follows:

$$F_{tr,Rpl} = min\left(F_{cwt}, F_{cfb}, F_{epb}, F_{bwt}, F_{bt}\right) \tag{3}$$

The full procedure is exemplified in [12] for the RJ specimen investigated in this paper. Another worked example of a beam-to-column joint with a bolted end-plate connection can be found in [2].

A reasonable estimation of the ultimate moment resistance of the joints M_{Ru} can be achieved by performing the same assembly procedure as described for M_{Rpl} using the ultimate resistances of components F_{Ru} instead of F_{Rpl}. It is worth noting that special attention has to be paid to the risk of instability in the components subjected to compression such as the column web in compression and the beam flange in compression.

3.2.3. Initial stiffness

The initial stiffness $S_{j,ini}$ characterises the rotational behaviour of a joint up to the limit of the elastic region. As long as the elastic resistance is not exceeded, the rotational stiffness depends solely on the initial rigidity of the joint basic components and is derived from the latter's elastic stiffnesses. The estimation of $S_{j,ini}$ is exemplified in Fig. 5 for the mechanical model of the RJ joint previously illustrated in Fig. 3.

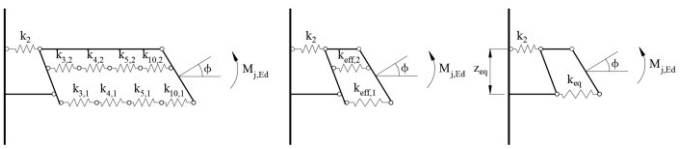

Fig. 5 Spring model for the evaluation of $S_{j,ini}$ for end-plated joints (RJ, EPB and CFB)

For an end-plated joint with two or more bolt-rows in tension, it is assumed that the deformations of the bolt rows are proportional to the distance to the centre of compression. The elastic forces in these rows depend on the stiffness of the components working as a series of springs k_i in the row in question. The deformations of each component can be added so that the series of individual springs k_i is replaced by a

Published in : Advanced Steel Construction (2022), vol. 18, no.3, pp. 679-686
DOI:10.18057/IJASC.2022.18.3.5
Status : Postprint (Author's version)

single spring with an effective stiffness $k_{eff,r}$ as shown in Fig. 5. Furthermore, these effective springs per bolt-row can be replaced by an equivalent spring k_{eq} acting at a distance z_{eq} from the centre of compression.

The assumptions described here above allow for the evaluation of the initial stiffness of the joint as follows:

$$S_{j,ini} = \frac{Ez^2}{\sum_i \frac{1}{k_i}} \tag{4}$$

where k_i is the elastic stiffness of the ith contributing component, z is the lever arm and E is the modulus of elasticity of steel.

Eq. (4) can be applied straightforwardly to joints with welded connections (as herein for BFC and CWC specimens), whilst for end-plated joints (RJ, EPB and CFB) additional parameters described above have to be determined using Eqs. (5)-(7):

$$k_{eff,r} = \frac{1}{\sum_i \frac{1}{k_{i,r}}} \tag{5}$$

$$z_{eq} = \frac{\sum_r k_{eff,r} h_r^2}{\sum_r k_{eff,r} h_r} \tag{6}$$

$$k_{eq} = \frac{\sum_r k_{eff,r} h_r}{z_{eq}} \tag{7}$$

The stiffness model depicted in Fig. 5 is defined in line with the provisions of Eurocode 3 Part 1-8. Its application has to be in compliance with the static theorem, ensuring the equilibrium between the internal forces distributed within the joint with the external bending moment. The assumed infinite transverse stiffness of the beam allows to apply the Bernoulli assumption and to fulfil the compatibility of displacements. As long as the elastic resistance of the constitutive springs is not reached, the plasticity criterion is met as well. In the same time, referring only to the elastic range of behaviour, the deformation capacity of the springs is not prone to limitations due to ductility requirements.

3.2.4. Strain-hardening stiffness

The elastic moment resistance M_{Rel} of the joints is conventionally considered as $2/3M_{Rpl}$. Beyond this limit, the behaviour of the joints becomes non-linear. To characterise this non-linear response, the stiffness of the joints may be derived from $S_{j,ini}$ by affecting the latter with a stiffness ratio μ. For endplated and welded connections, provided that the bending moment M_j varies between M_{Rel} and M_{Rpl}, this assumption allows to approximate the rotational stiffness to $S_{j,ini}/7$, as illustrated in Fig. 6 (a).

The approach proposed in Eurocode 3 enables the user to estimate with a reasonable accuracy the initial stiffness $S_{j,ini}$ (up to M_{Rel}) and the secant stiffness which characterises the rotational behaviour of the joint up to M_{Rpl}. Beyond its plastic moment resistance, the joint is assumed to exhibit no rotational stiffness, leading thus to a conservative idealisation of its post-plastic response. This general-purpose idealisation is

Published in : Advanced Steel Construction (2022), vol. 18, no.3, pp. 679-686
DOI:10.18057/IJASC.2022.18.3.5
Status : Postprint (Author's version)

acceptable for common design practises, whilst for specific cases where a precise prediction of the post-plastic behaviour is sought, it is insufficient.

Based on the analytical expressions reported here above, the strainhardening stiffness $S_{j,st}$ may be derived based on the strain-hardening stiffness coefficients k_{st} of the individual basic components. In [8], the authors propose an assembly procedure for the assessment of $S_{j,st}$. This allows for the characterisation of the post-plastic behaviour of the joints beyond the plastic moment resistance M_{Rpl} up to the ultimate one M_{Ru} as depicted in Fig. 6 (b).

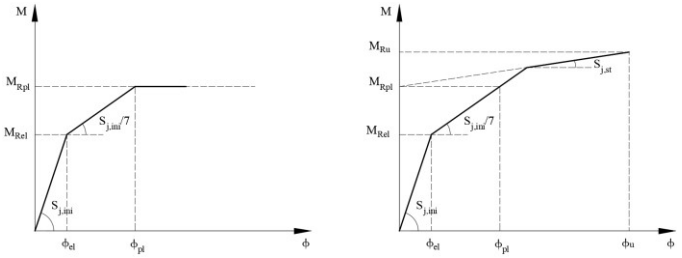

(a) According to Eurocode 3 (b) According to Jaspart et al [8]

Fig. 6 Rotational stiffness of joints

The assembly procedure relies on the relative importance of the plastic moment resistance $M_{Rpl,comp,i}$ of each individual basic component when compared to the plastic resistance M_{Rpl} of the joint. For all active components, $M_{Rpl,comp,i}$ is calculated by considering the ith component as being the only one active within the joint. Once evaluated for each isolated component, $M_{Rpl,comp,i}$ is compared to the plastic moment resistance of the whole joint M_{Rpl}. Components with $M_{Rpl,comp,i}$ considerably higher than M_{Rpl} are assumed to contribute in an elastic way to $S_{j,st}$. Contrarily, the components with $M_{Rpl,comp,i}$ closer to M_{Rpl} would undergo plasticity and, implicitly, strain-hardening effects would develop in the components affecting thus the $S_{j,st}$. Therefore, the evaluation of $S_{j,st}$ implies a classification of the components according to their own plastic resistance with a view to identifying the components contributing to $S_{j,st}$ by means of their initial elastic stiffness coefficient k_i and the ones contributing with their strain-hardening stiffness coefficient k_{st} assumed to be equal to $k_i/50$. A boundary value of the moment capacity has been proposed by Jaspart [1] after extensive studies of experimental tests on end-plated joints as follows in Eq.8.

$$M_{Rpl,limit} = 1.65 M_{Rpl} \tag{8}$$

Accordingly, a component with $M_{Rpl,comp,i} > M_{Rpl,limit}$ is considered to remain in its elastic range of behaviour, therefore having an elastic contribution to $S_{j,st}$. Conversely, when $M_{Rpl,comp,i} \leq M_{Rpl,limit}$, the ith component contributes to $S_{j,st}$ with its strain-hardening stiffness. The strain hardening stiffness of the joint $S_{j,st}$ is estimated in the following way:

$$S_{j,ini} = \frac{Ez^2}{\sum \frac{1}{k^*}} \tag{9}$$

where:

$$\sum \frac{1}{k^*} = \sum_m \left(\frac{1}{k_{i,m}}\right)_{M_{Rpl,comp,i} > M_{Rpl,limit}} + \sum_k \left(\frac{1}{k_{st,k}}\right)_{M_{Rpl,comp,i} \leq M_{Rpl,limit}} \tag{10}$$

with k and m - indices for components.

Published in : Advanced Steel Construction (2022), vol. 18, no.3, pp. 679-686
DOI:10.18057/IJASC.2022.18.3.5
Status : Postprint (Author's version)

3.2.5. Rotation capacity

Limited guidance on the assessment of the rotation capacity of joints ϕ_{Cd} is provided in the current version of Eurocode 3. Rules to assure adequate rotation capacity for joints with bolted and welded connections are given as general requirements meant to avoid brittle failures associated to the rupture of bolts or weld failure. The few guidelines related to the assessment of ϕ_{Cd} lead to a rather qualitative estimation of it. However, an alternative method to quantify the rotation capacity may be contemplated on the basis of the procedure described here above. Referring to Fig. 6 (b), the ultimate rotation capacity ϕ_u, i.e. the rotation of the joint corresponding to its ultimate resistance may be readily estimated on the basis of M_{Rpl}, M_{Ru} and $S_{j,st}$ in the following manner:

$$\emptyset_u = \frac{M_{Ru} - M_{Rpl}}{S_{j,st}} \tag{11}$$

Similarly, the plastic rotation ϕ_{pl} is given by:

$$\emptyset_{pl} = \frac{3M_{Rpl}}{S_{j,ini}} \tag{12}$$

4. Finite element simulations

Physical tests conducted on full-scale specimens represent the most reliable method of assessment of the full non-linear behaviour of steel joints. However, such practices are in general economically inefficient and challenging to perform due to the limitations of available instrumentation. Moreover, experimental testing may be irrelevant for the investigation of local effects (i.e. stress distribution, prying and contact forces etc.) due to the difficulty to be measured with sufficient accuracy in reality. To overcome these challenges, numerical simulations are frequently used in the investigation of steel joints subjected to various types of loads. Hereafter, FE Analyses are employed in the evaluation of the M_j - ϕ curve of steel joints subjected to quasi-static loads. The objective is to assess the potential and the accuracy of FE solutions in reproducing the complex non-linear behaviour of the joints.

4.1. FE models description and modelling assumptions

The joint configurations addressed in this paper were modelled in a 3D numerical environment using specific FE modelling techniques. The FE models were developed using the commercial software Abaqus/CAE [13]. For static analyses, the iterative Newton-Raphson method is used to solve the non-linear equilibrium equations in Abaqus/Standard.

Referring to Fig. 1, the symmetry of the test assemblies in terms of geometry, loading, and boundary conditions is easily noticeable. By exploiting this symmetry, only 1/4th of the physical specimen was explicitly modelled, thus allowing for the reduction of the computational effort. This modelling assumption was used to build the FE models of the four joints (RJ, EPB, CFB and BFC) in which no instability phenomena occurred in the experimental tests. Due to the unsymmetrical behaviour of the CWC specimen associated to the instability in the column web, the full assembly was numerically modelled so that the geometrical imperfections are properly taken into account.

Published in : Advanced Steel Construction (2022), vol. 18, no.3, pp. 679-686
DOI:10.18057/IJASC.2022.18.3.5
Status : Postprint (Author's version)

Three-dimensional solid C3D8R 8-node linear brick elements with reduced integration were used to model the main structural parts as shown in Fig. 7. Exceptions were made for the welds and the root radius regions of the I and H sections, for which C3D6 wedge elements were used. The welds were modelled as parts with triangular cross-section. The threads of the bolts were not explicitly modelled; hence the bolts were modelled as having a smooth shank with a diameter of 14.1 mm which would simulate the resistant area in the threaded region.

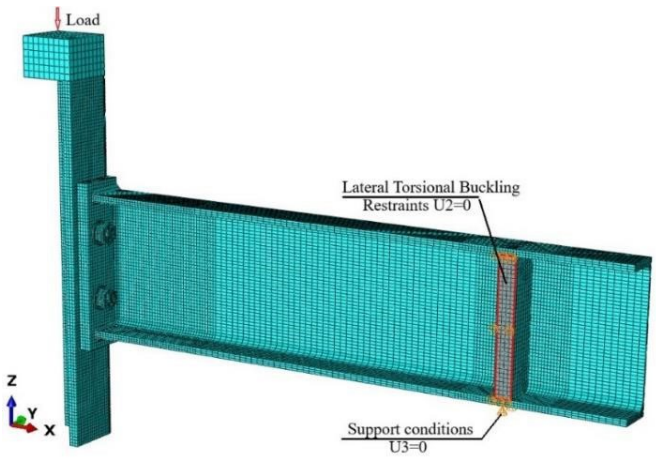

Fig. 7 3D view of the FE model (RJ specimen)

Fig. 8 depicts the mesh density for specific parts of the model. A dense mesh was assigned to the regions where local effects are likely to occur. Therefore, the end-plate, the bolts, and the region in the immediate proximity of the connection were discretised using small-size elements. Generally, a minimum number of 3 elements over the thickness was assigned for all plates of the model. Mesh seeds of 4 mm were applied to the parts in the regions with high density mesh, excepting the bolts for which mesh seeds of 2 mm were used.

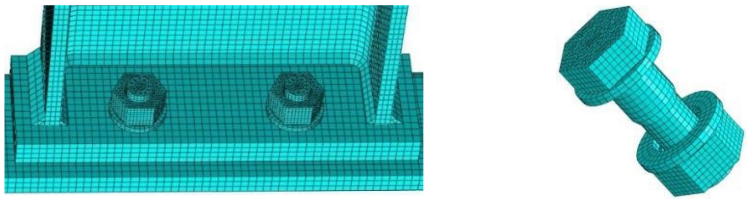

(a) End-plate region (b) Bolt part

Fig. 8 Mesh density

The entire model was composed of approximately 60 000 elements and, because the simulations provided results that agreed with the experimental data, the mesh density was considered to be adequate. Additionally, several mesh sensitivity studies were conducted, and it has been demonstrated that an enhanced mesh refinement would minimally affect the global response.

4.2. Materials

The non-linear behaviour of steel was implemented in the FE models through a non-linear stress-strain relationship with material hardening. Damage evolution or failure criteria were not explicitly implemented in the material model. The stress-strain constitutive relationships were derived from tensile coupon tests

Published in : Advanced Steel Construction (2022), vol. 18, no.3, pp. 679-686
DOI:10.18057/IJASC.2022.18.3.5
Status : Postprint (Author's version)

conducted on samples extracted from the plates of the specimens. For the elastic range of behaviour, a modulus of elasticity E=210 GPa was considered for all materials, whilst the yield stress σ_y was assigned to each material based on the data reported in Table 2.

The engineering stress-strain (σ_{eng} - ε_{eng}) curves generated throughout the tests were converted into true stress-logarithmic plastic strain (σ_{true} - ε_{pl}) curves. The latter served as constitutive laws for the post-plastic behaviour of the materials allowing to consider adequately the strain-hardening of steel. To convert the σ_{eng} - ε_{eng} curves into the corresponding σ_{true} - ε_{pl} ones, reference is made to Eqs. (13)-(15).

$$\sigma_{true} = \sigma_{eng}\left(1 + \varepsilon_{eng}\right) \tag{13}$$

$$\varepsilon_{true} = 1\mathrm{n}\left(1 + \varepsilon_{eng}\right) \tag{14}$$

$$\varepsilon_{pl} = \varepsilon_{true} - \frac{\sigma_{true}}{E} \tag{15}$$

4.3. Loading and boundary conditions

The support conditions provided by the test setup were replicated in the FE environment by defining specific boundary conditions. The beam is simply supported at one of its end, hence the vertical displacement (U_3) has been restrained at the positon of the support as shown in Fig. 7. Additional supports were provided laterally to the stiffeners welded to the beam in order to prevent the loss of stability and the lateral torsional buckling of the beam. Since the initial modelling assumption was based on the symmetry of the system, appropriate symmetry conditions were applied on the two symmetry planes. A displacement control option was used in the FE simulations to mimic the monotonic load applied on the column top. The bolts were only snug tightened in reality, hence the pre-tensioning of the bolts was not considered.

To simulate the local buckling of plates occurring during the experimental test conducted on the CWC specimen, initial imperfections were implemented in the numerical model. A linear buckling analysis (LBA) was performed in order to evaluate the relevant buckling modes. The eigenvalues of these buckling modes were used further in a post-buckling analysis performed under the assumption of having initial imperfections with a magnitude of d/200, where *d* is the clear depth of the column.

4.4. Interaction and contact

The interaction between the constitutive parts of the FE model was simulated through imposed constraints and contact conditions. Tie constraints were used to connect the elements between which relative displacements are not allowed. Accordingly, this type of constraint was used to connect: the weld to the beam/end-plate/column, the beam to the end-plate/column, the stiffeners to the beam/column, and the loading plate to the column.

A surface-to-surface type of contact was defined for the interaction of several contact pairs such as: the bolt-heads with the end-plate, the bolt-shank with the bolt-holes in the end-plate and column flange, the nuts with the column flange, and the end-plates with the column flange. The behaviour for the normal direction was defined using a "Hard contact" property, so that the interpenetration of the surfaces in contact is not allowed. For the tangential direction, a Coulomb friction model with a penalty formulation was applied. A friction coefficient of 0.3 was assumed for all contact pairs of the model.

Published in : Advanced Steel Construction (2022), vol. 18, no.3, pp. 679-686
DOI:10.18057/IJASC.2022.18.3.5
Status : Postprint (Author's version)

5. Results and discussion

In order to validate the methods of assessment presented in the previous sections, a comparison between the results is provided hereafter. The efficiency of analytical and numerical approaches is evaluated by confronting the results in terms of M_j - ϕ curves for all five joint configurations. An additional validation criterion concerns the failure mode or the failing components of the joints. A comparison between the numerical values of the key parameters characterising the behaviour of the joints is reported in Table 5. The elastic moment resistance M_{Rel} is chosen as a reference due to its convenience of being detectable visually on the experimental M_j - ϕ curve. Thorough presentations and discussion of the results for each individual joint are provided in the following sections.

Table 5
Results comparison for the key parameters

Parameter	Assessment method	Specimens				
		RJ	EPB	CFB	BFC	CWC
M_{Rel} [kNm]	Experimental	26.47	18.89	28.64	67.65	25.23
	Analytical	25.92	17.02	26.01	71.99	27.95
	FE simulation	27.81	19.02	28.07	69.57	37.27
M_{Ru} [kNm]	Experimental	47.23	38.48	50.85	91.69	43.40
	Analytical	44.75	31.56	44.74	91.85	41.92
	FE simulation	44.72	36.78	50.37	95.03	48.81
$S_{j,ini}$ [kNm/rad]	Experimental	3267.9	1749.1	3719.5	35077	19584
	Analytical	5107.2	3058.6	5392.9	∞	16765
	FE simulation	3271.8	1811.4	3598.7	38650	26683
$S_{j,st}$ [kNm/rad]	Experimental	383.94	104.24	140.11	284.2	N/A
	Analytical	102.13	436.94	107.86	0.0000	N/A
	FE simulation	66.826	90.653	83.991	160.19	N/A
ϕ_{el} [rad]	Experimental	0.0081	0.0108	0.0077	0.0032	0.0018
	Analytical	0.0051	0.0056	0.0048	0.0000	0.0017
	FE simulation	0.0085	0.0105	0.0078	0.0018	0.0014
ϕ_u [rad]	Experimental	0.0739	0.1172	0.0728	0.0891	0.0058
	Analytical	0.0611	0.0631	0.0572	N/A	0.0075
	FE simulation	0.0744	0.1151	0.0809	0.1046	0.0038

5.1. Test 1: RJ specimen

Fig. 9 illustrates the comparison between the M_j - ϕ curves obtained through experimental, analytical, and numerical methods for the RJ specimen. The method proposed in this paper leads to a prediction in good agreement with the experimental results, even though the initial rotational stiffness $S_{j,ini}$ is somewhat overestimated. The representative limits for the moment resistance (M_{Rel}, M_{Rpl} and M_{Ru}) and the post-elastic stiffness ($S_{j,ini}/7$ and $S_{j,st}$) are estimated with a satisfactory precision, shaping thus a tri-linear M_j - ϕ curve with a high degree of reliability. For this specimen, the analytical prediction of the rotation capacity is similar to the actual value, hence the ductility of the joint is reasonably estimated as well. The failure mode analytically predicted corresponds to the failure of the column flange in bending (cfb) with plastic deformations in the end-plate in bending (epb) and in the column web in compression (cwc). The same failure mode has been observed in reality, the column flange exhibiting clear evidences of plasticity at the level of the first bolt row in tension. As expected, the differences between the Eurocode 3 method and the approach proposed in this paper are noticeable only for the post-plastic range. Given the fact that the joint's plastic moment resistance is limited by the resistance of the column flange in bending (cfb), no estimation

Published in : Advanced Steel Construction (2022), vol. 18, no.3, pp. 679-686
DOI:10.18057/IJASC.2022.18.3.5
Status : Postprint (Author's version)

of the rotation capacity of the joint can be established with the standard method as, in Eurocode 3, this component is assumed to be infinitely ductile. Note that, for the sake of completeness, the extent of the plateau represented with a dashed red line in Fig. 9 has been arbitrarily set, what represents an assumption for all the cases investigated hereafter.

The numerically derived M_j - ϕ curve is as well in a good agreement with the experimental one. The initial stiffness $S_{j,ini}$ is estimated with a remarkable accuracy, whilst for the post-plastic range, the numerical prediction seems to underestimate slightly the rotational stiffness. The decrease in the post-plastic stiffness $S_{j,st}$ can be explained based on the plastic deformations developed within the joint. The equivalent plastic strain distribution shows that the column flange undergoes plastic deformations up to its failure, losing gradually its stiffness. Therefore, the failure mode can be associated to the column flange in bending component, this being in compliance with the experimental and analytical results.

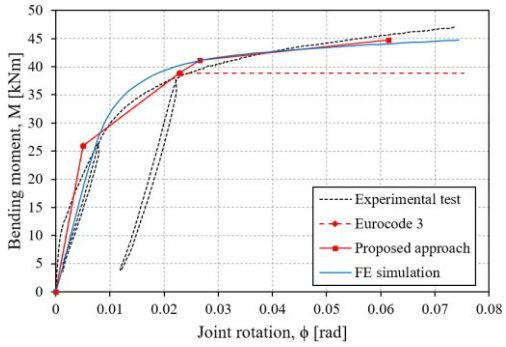

Fig. 9 Results comparison – RJ specimen

5.2. Test 2: EPB specimen

The results reported in Fig. 10 show that the proposed method provides a rather conservative prediction for the ultimate bending resistance and for the ultimate rotation capacity of the EPB joint. Otherwise, the analytical prediction follows closely the real behaviour of the joint, leading to an acceptable estimation of the elastic/plastic moment resistances and of the secant/strain-hardening stiffnesses. The significant discrepancy between the analytical prediction and the real behaviour may be attributed to the limitations of the equivalent T-stub model used to characterise the end-plate in bending component. In this case, the end-plate in bending (epb) is the failing component and governs the global behaviour of the joint. Due to its relatively small thickness of 8 mm, the end-plate can fall into the category of "thin" plates if compared to the conventional range of thicknesses for such joint parts. The T-stub model may be well-calibrated for plates with thicknesses in the usual range, yet it underestimates the extent of the plastic yield mechanism (for Failure mode 1) or of the yield lines in the component (for Failure mode 2) when applied to thinner plates as already highlighted in [14]. These aspects remain to be addressed in further investigations on the improvement of the equivalent T-stub model proposed in Eurocode 3 Part 1-8.

Published in : Advanced Steel Construction (2022), vol. 18, no.3, pp. 679-686
DOI:10.18057/IJASC.2022.18.3.5
Status : Postprint (Author's version)

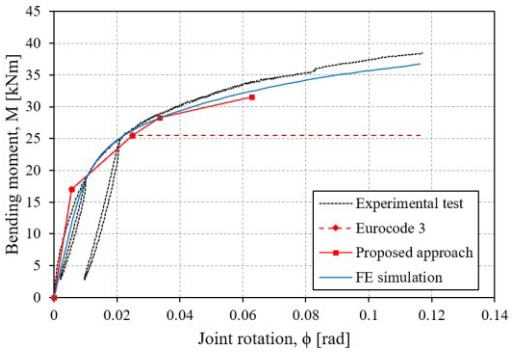

Fig. 10 Results comparison – EPB specimen

The FE simulation provides a prediction with a good accuracy. The main characteristics of the non-linear behaviour of the joint are well estimated; only the ultimate moment resistance is marginally underrated. The failure mode corresponds to the failure of the end-plate in bending in the region of the first bolt row in tension where significant concentration of plastic deformations is localised. The failure of the same joint component was observed during the experimental test, thus validating the FE model.

5.3. Test 3: CFB specimen

A conservative prediction for the M_j - ϕ curve of the CFB specimen is obtained with the analytical approach (see Fig. 11). The ultimate moment resistance is significantly underestimated, whereas an acceptable prediction for the rotational stiffness is observed (note the parallelism between the strain-hardening branches). Since the analytically predicted failing component is the column flange in bending, what is in line with the test observations, the difference between the results may be once again linked to the limitations of the T-stub model on which the characterisation of the component relies.

A very good agreement is noticed between the results acquired from the test and the ones provided by the numerical simulation. The FE model replicates with a high accuracy the response of the physical specimen, all the validation criteria enounced previously being met.

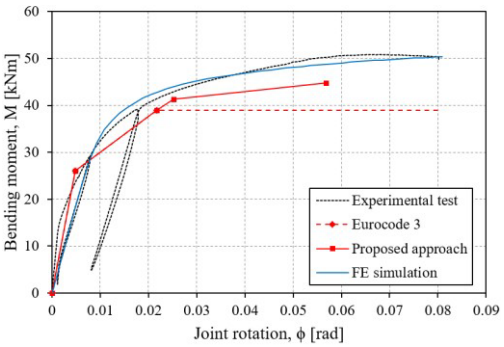

Fig. 11 Results comparison – CFB specimen

5.4. Test 4: BFC specimen

The component method provides only a partial prediction for the M_j - ϕ curve for the BFC joint. The peculiarity of this specimen is that it was designed in such a way that the "deemed-to-fail" component would be the beam flange and web in compression (bfc). Therefore, the global response of the joint is characterised solely by the behaviour of this particular component which, as a matter of fact, is the only

Published in : Advanced Steel Construction (2022), vol. 18, no.3, pp. 679-686
DOI:10.18057/IJASC.2022.18.3.5
Status : Postprint (Author's version)

one active within the joint. Referring to the provisions of Eurocode 3, this component is assumed to exhibit an infinite initial stiffness. As long as the elastic range of behaviour is investigated, Fig. 12 shows that this assumption leads to satisfactory results. On the other hand, the characterisation of the post-plastic behaviour of the joint raises specific challenges. For class 1 and 2 cross-sections, the plastic resistance is expected to be reached without the occurrence of local buckling phenomena. An IPE 180 section is classified as a class 1 cross-section which can undergo plastic deformations beyond its plastic resistance. This allows to estimate the ultimate bending resistance of the BFC joint with a rather good precision. The strain-hardening stiffness and the ultimate rotation capacity have to be derived based on the characteristics of the beam as well. However, since the behaviour of members is outside the scope of this paper, an arbitrary "expectable" value for the ultimate rotation capacity of the joints is assumed here.

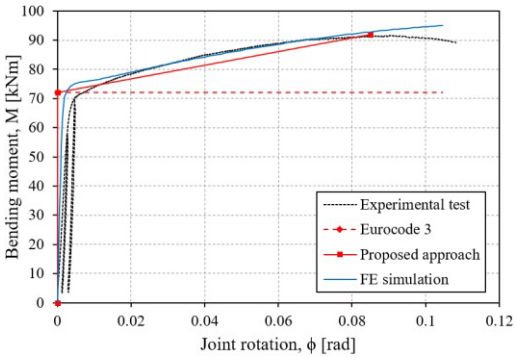

Fig. 12 Results comparison – BFC specimen

The shortcoming of the analytical method can be overcome by conducting a FE analysis. This tool proves to be very reliable, the numerical prediction being very similar to the actual behaviour of the BFC specimen.

5.5. Test 5: CWC specimen

Observations of the experimental test on the CWC specimen indicate a failure mode associated to the buckling of the column web (cwc), which is a non-ductile failure mode. Once the buckling resistance of this component is reached, the failure of the whole joint occurs without any resistance reserve. Therefore, the joint's bending resistance corresponding to the buckling of the column web would represents the "plastic" and the "ultimate" moment resistance as well. This means that the Eurocode 3 approach and the method introduced in this paper would lead to identical results, hence, only the results for the standard approach are reported in Fig. 13.

Due to complexity related to instability phenomena, the rules prescribed by Eurocode 3 are intended to cover the most unfavourable scenarios so that, in common design practice, the resistance of components in compression under instability would not be overestimated. Accordingly, the design standard addresses this issue by assuming extreme or maximum-expected initial imperfections introduced in computations by means of buckling reduction factors ρ. Fig. 13 illustrates the very conservative $M_j - \phi$ curve of the CWC joint estimated using the buckling reduction factors set by the standard. If the influence of these initial imperfections is disregarded (ρ=1), the analytical prediction is enhanced and somewhat in a better agreement with the real behaviour of the CWC joint but reflects an unrealistic situation.

Published in : Advanced Steel Construction (2022), vol. 18, no.3, pp. 679-686
DOI:10.18057/IJASC.2022.18.3.5
Status : Postprint (Author's version)

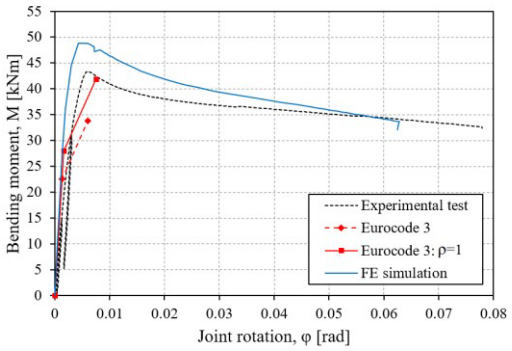

Fig. 13 Results comparison – CWC specimen

The FE post-buckling analysis conducted on the CWC numerical model leads to results in partial agreement with the experimental data. The numerical prediction captures well the initial elastic stiffness of the joint, yet it overestimates by 12% the buckling load. This discrepancy may arise from the inadequate consideration of initial imperfections in the FE model or from the fact that, in reality, the load could be applied with a small eccentricity, thus inducing a parasitic bending moment that leads to a further reduction in the buckling capacity of the column web (cwc).

As main outcome, it can be concluded that further investigations are required for this joint component in view of improving the accuracy of the analytical formulation presently proposed in the standard for the prediction of its resistance.

6. Conclusions

Analytical and numerical methods have been employed to investigate the behaviour of beam-to-column steel joints under quasi-static loading. Predictions for five joint configurations were compared with experimental data, thus assessing the reliability of the two approaches. The analytical procedure proposed for the estimation of the full non-linear behaviour of joints is to be seen as an extension of the component method implemented nowadays in Eurocode 3 Part 1-8. Its application yields relevant results, allowing a more accurate and realistic prediction of the joint properties to be used in non-linear structural analysis. FE simulations of physical tests have been performed in a three-dimensional numerical environment. Generally, the simulations captured with a good accuracy the behaviour of the joints investigated in this paper. The following essential observations and conclusions may be drawn:

(1) The analytical approach based on the component method represents an interesting tool for the assessment of the non-linear response of steel joints subjected to quasi-static loads. The results reported in this paper are in a partialto-good agreement with the experimental data despite the simplifying assumptions of the method. The rather tedious computational process can be readily dealt with by developing comprehensive computational routines in any available mathematical solver.

(2) When applied to thin plates, the equivalent T-stub model integrated in the current version of Eurocode 3 leads to conservative predictions of the ultimate moment resistance of joints. Further investigations on its sensitivity to the thickness of plates have to be carried out. Such studies are conducted currently at the University of Liège aiming at enhancing the accuracy of the equivalent T-stub model.

(3) The prediction of the resistance of the "Column Web in Compression" component as presently recommended in Eurocode 3, Part 1-8, is very conservative. As for the previous point, further investigations

have to be conducted in order to improve the accuracy of the existing models. Such studies are also conducted currently at the University of Liège.

(4) The reliability of the proposed approach is highly dependent on the characterisation of basic components. To ensure an accurate prediction for the behaviour of a joint, the geometrical and mechanical properties of its active components must be rigorously assessed. Some of the analytical expressions proposed for this purpose still require additional investigations and in-depth studies of basic components' behaviour.

(5) FE simulations represent a very reliable alternative to experimental testing, even though they are still computationally expensive and require a set of skills and knowledge around FE solutions and modelling techniques.

(6) A special attention has to be paid when simulating the behaviour of joints in which instability phenomena are likely to occur. The initial imperfections and/or the possible eccentricities in the load application have to be meticulously accounted for in the FE model.

Acknowledgements

Part of the presented work was carried out with a financial grant from the Research Fund for Coal and Steel of the European Community (Robustimpact project - Grant N° RFSR-CT-2012-00029).

References

[1] Jaspart J.-P., "Etude de la semi-rigidité des noeuds poutre-colonne et son influence sur la résistance et la stabilité des ossatures en acier", PhD Thesis, University of Liège, Liège, Belgium, 1991.

[2] Jaspart J.-P. and Weynand K., Design of joints in steel and composite structures, ECCS Eurocode Design Manual, Wiley, Ernst & Sohn, 2016.

[3] Da Silva L. S., "Towards a consistent design approach for steel joints under generalized loading", Journal of Constructional Steel Research, vol. 64, no. 9, 1059–1075, 2008.

[4] EN 1993-1-8, Eurocode 3 - Design of steel structures - Part 1-8: Design of joints, Brussels: European Committee for Standardisation, 2005.

[5] Francavilla B. A., Latour M., Rizzano G., Jaspart J.-P. and Demonceau J.-F., "On the robustness of earthquake-resistant moment-resistant frames: influence of innovative beam-to-column joints", Open Construction and Building Technology Journal, vol. 12, 2018

[6] Kuhlmann U., Jaspart J. P., Vassart O., Weynand K. and Zandonini R., "Robust structures by joint ductility", RFCS Publishable Report, 2008.

[7] Demonceau J.-F. and Jaspart J.-P., "Experimental test simulating a column loss in a composite frame", Advanced Steel Construction, vol. 6, no. 3, 891–913, 2010.

[8] Jaspart J.-P., Corman A. and Demonceau J.-F., "Ductility assessment of structural steel and composite joints", 2019.

[9] Kuhlmann U. *et al.*, Robust impact design of stel and composite building structures (RobustImpact), European Commission, 2017.

[10] Demonceau J.-F., Vanvinckenroye H., D'Antimo M., Denoël V. and Jaspart J.-P., "Beam-to-column joints, column bases and joint components under impact loading", ce/papers, vol. 1, no. 2–3, 3890–3899, 2017.

[11] Hoffmann N. *et al.*, "RobustImapct: Deliverable D.5a. Detailed results of the experimental tests", 2016.

[12] Golea T., "Behaviour of steel joints under dynamic actions", Master Thesis, University of Liège, Liège, Belgium, 2020.

[13] Dassault Systèmes, "ABAQUS", 2016.

[14] Demonceau J.-F., "Steel and composite building frames: sway response under conventional loading and developmet of membrane effects in beams further to an exceptional action", PhD Thesis, University of Liège, Liège, Belgium, 2008.